Proceedings World Geothermal Congress 2020+1
Reykjavik, Iceland, April - October 2021

Estimating *in Situ* Rock Mass Strength and Elastic Modulus of a Geothermal Reservoir

Marlène C. Villeneuve[1], Michael J. Heap, Alexandra R. L. Kushnir and Patrick Baud

[1]Department of Geological Sciences, University of Canterbury, Private Bag 4800, Christchurch 8140, New Zealand

marlene.villeneuve@canterbury.ac.nz

Keywords: Geological Strength Index, fractures, core, well

ABSTRACT

Knowledge of the strength and elastic modulus of a reservoir rock is important for the optimisation of the geothermal resource, but is rarely considered during exploration and rock characterisation studies. This is especially true over intervals with high fracture densities, where the rock mass strength and stiffness will be significantly lower than the intact rock strength and stiffness. Here we apply rock engineering techniques for assessing rock mass strength and stiffness to the reservoir rock for the geothermal systems in the Upper Rhine Graben, such as those at Soultz-sous-Forêts and Rittershoffen (both France). We couple uniaxial and triaxial deformation experiments performed on intact rock with Geological Strength Index assessments—using the wealth of information from core and borehole analyses—to derive the generalised Hoek–Brown failure criterion and provide rock mass strength and elastic modulus estimates for the granite reservoir and overlying sandstone rocks at Soultz-sous-Forêts (from a depth of 1012 to 2200 m).

The fracture densities in this reservoir granite range up to ~ 30 fractures/m. The average intact uniaxial compressive strength (UCS) and elastic modulus of the granite are 140 MPa and 40 GPa, respectively, while for the dry sandstone they range from 50-250 MPa and 10-40 GPa, respectively, depending on the unit. Intact strength increases with confining pressure (i.e. depth). For the granite, the intact UCS is quite homogeneous. The modelled strength of the intact granite is 360 MPa at a depth of 1400 m and increases to 455 MPa at a depth of 2200 m (using our estimate for the empirical m_i term of 30, determined using triaxial and tensile strength measurements on the intact granite). For the sandstone, intact UCS is highly variable, and while it also increases with confining pressure, this does not translate to a direct relationship with depth because the UCS is unit-dependent, and the unit strengths decrease with depth. The depth-correct intact rock strength of the dry sandstone varies from 150-350 MPa (using an m_i of 19).

Strength of the rock masses vary in accordance with the intact strength, the fracture density and the extent and nature of the fracture infill, reaching lows of ~ 30 MPa (in, for example, the densely fractured sandstone in exploration well EPS-1 (at Soultz-sous-Forêts) at a depth of ~ 1115 m) and highs of above 400 MPa (in, for example, the largely unfractured granite at a depth of ~ 1940–2040 m). Variations in rock mass elastic modulus are qualitatively similar (values vary from 1 to 2 GPa up to the elastic modulus of the intact rock, 40 GPa).

Our study highlights that macrofractures and joints reduce rock mass strength and elastic stiffness and should be considered when assessing the rock mass for well stability and rock mass deformation due to stress and pressure redistribution in the reservoir. We present this case study to demonstrate how a simple and cost-effective engineering method can be used to provide an indication of the *in situ* strength and elastic modulus of reservoir rock masses, important for a wide range of modelling and stimulation strategies. We recommend that the effect of macrofractures on rock mass strength and stiffness be validated for incorporation into geomechanical characterisation for geothermal reservoirs worldwide.

1. INTRODUCTION

Geothermal projects in the Upper Rhine Graben (URG)—a Cenozoic rift valley that runs along the border between France and Germany—aim to harness thermal gradient anomalies (100 °C/km) attributed to hydrothermal circulation within the fractured Palaeozoic granitic basement and the overlying Permian and Triassic sediments (Pribnow and Schellschmidt, 2000; Guillou-Frottier et al., 2013; Magnenet et al., 2014).

Further, and pertinent to this study and many geothermal reservoirs, the high fracture densities within the URG reservoirs—reaching up to ~30 fractures/m (Genter and Traineau, 1996)—question the direct applicability of deformation experiments performed in nominally intact rock (as discussed in Richards and Read, 2007). In these intensely fractured zones, the contribution of the fractures to the rock mass strength and stiffness must be considered in geotechnical practices.

We provide here estimates of the *in situ* rock mass strength (using the generalised Hoek-Brown criterion commonly used in engineering; Hoek et al., 2002) and rock mass elastic modulus (using the Hoek-Diederichs equation; Hoek and Diederichs, 2006) for the granite reservoir and overlying sandstone units at Soultz-sous-Forêts. These values are crucial input parameters for reservoir-scale modelling (e.g., Bérard and Cornet, 2003; Yoon et al., 2013; McClure and Horne, 2013 and references therein) and guiding stimulation design (e.g., Cipolla et al., 2008; Meller and Ledésert, 2017). The materials used for this study were taken from exploration borehole EPS-1 from the Soultz-sous-Forêts geothermal site (Figure 1).

This paper highlights the work from two studies: Villeneuve et al. (2018) and Heap et al. (2019) which provide a procedure for starting with intact rock strength and stiffness measurements, followed by a rock mass characterisation using published borehole studies and combining these to derive rock mass strength and stiffness estimates at the borehole scale (from a borehole depth of ~1012 to ~2200 m in EPS-1). The objective is to highlight the effect of macrofractures on rock mass strength and stiffness, even at the borehole scale, and to demonstrate that modelling the rock mass using only intact rock strength and stiffness parameters has the potential to overestimate these values.

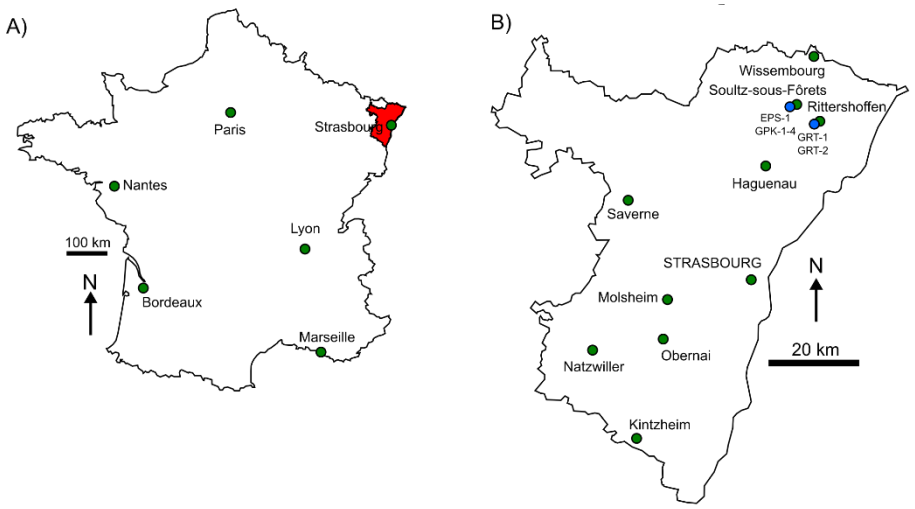

Figure 1: A) Map of France showing the location of the Bas-Rhin department of Alsace (in red). B) Map of the Bas-Rhin department of Alsace (shown in red in panel A) showing the location of the major cities/towns and the geothermal sites and geothermal boreholes of Soultz-sous-Forêts and Rittershoffen. Modified from Heap et al. (2017).

2. MATERIALS AND METHODS

2.1 Upper Rhine Graben Reservoir Rocks

This Permian and Triassic Buntsandstein lithostratigraphic unit directly overlies the fractured Palaeozoic Upper Rhine Graben porphyritic granite reservoir. The sandstone units were sampled at twelve ~40–50 meter-spaced intervals (between 1008 to 1414 m; Heap et al., 2019) from the EPS-1 exploration well at the Soultz-sous-Forêts geothermal site (Figure 1). The petrophysical characterisation of the Buntsandstein can be found in Griffiths et al. (2016), Heap et al. (2017, 2018, 2019), and Kushnir et al. (2018). These were complemented with samples prepared from blocks (all from the Buntsandstein) acquired from local quarries (Heap et al., 2019). Four or five cylindrical samples, 20, 18.75, or 12 mm in diameter (depending on the strength of the sandstone), were cored from each of the twelve intervals sampled and precision-ground to a nominal length of 40, 37.5, or 24 mm, respectively. Samples from the quarry blocks were cored perpendicular to bedding to a diameter of 20 mm and precision-ground to a nominal length of 40 mm. Seventeen cylindrical granite samples (40 mm in diameter) were prepared from the cores collected (two from the 1420 m sample, 12 from the 1558 m sample, and three from the 1915 m sample from the EPS-1 exploration well) and precision-ground to a nominal length of 80-85 mm (Villeneuve et al., 2018). All of the samples were washed using tapwater and then dried in a vacuum oven at 40 °C for at least 48 h.

The samples were deformed under uniaxial and triaxial conditions at strain rates of 1.0×10^{-6} s^{-1} or 1.0×10^{-5} s^{-1} (for the sandstone and granite, respectively) until macroscopic failure. The load was measured using a load cell and the displacement was measured using either an LVDT or an extensometer (for the sandstone and granite, respectively). The measured load and displacement were then converted to stress and strain using the sample dimensions. See Heap et al. 2019 and Villeneuve et al. 2018 for additional details.

2.2 Hoek-Brown Failure Criterion for Intact Rocks

The Hoek-Brown failure criterion for intact rock provides a non-linear fit to triaxial data according to:

$$\sigma_1' = \sigma_3' + C_0 \left(m_i \frac{\sigma_3'}{C_0} + 1 \right)^{0.5} \quad \textbf{(1)}$$

where σ_1' and σ_3' are the effective maximum and minimum principal stresses, respectively, in MPa; C_o is the uniaxial compressive strength, in MPa, and m_i is a unitless empirical fitting parameter related to the lithology (Eberhardt, 2012). The two unknowns in Equation 1 are C_o and m_i. The uniaxial and triaxial test data were used to determine the C_0 and m_i for each sandstone and granite unit according to Eberhardt (2012) and Hoek and Brown (2018) using the computer software RocData from RocScience.

2.3 Rock Mass Characterisation

The nature of the rock mass was quantified using the Geological Strength Index (GSI), as described in Hoek and Brown (1980, 2018). This method uses a chart (Figure 2) to assign a category to the rock mass structure and the condition of the discontinuities. The GSI is quoted as a range because of its uncertainty and subjectivity. We used single, average values to describe the rock masses, but these are based on ranges, as shown in the ellipses in Figure 2 corresponding to a A) fair, B) excellent and C) poor rock mass in the URG granite (Villeneuve et al., 2018).

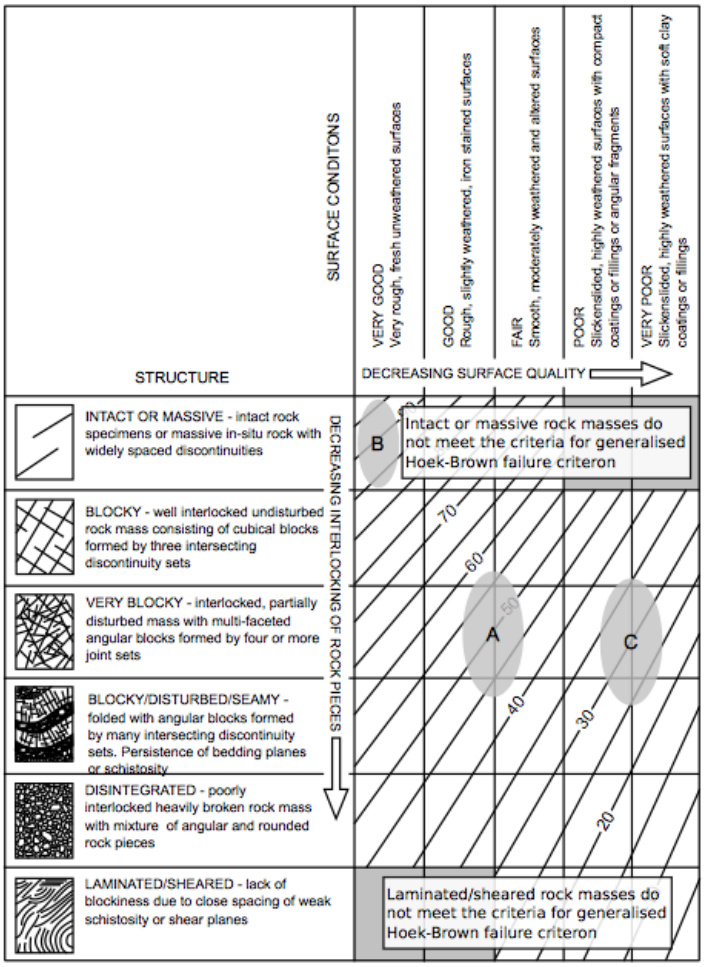

Figure 2: Chart for obtaining geological strength index (GSI). The positions of the three 25 m-interval rock masses from Soultz-sous-Forêts are shown on the chart (the three grey ellipses). Modified from Marinos et al. (2005) and Villeneuve et al. (2018). Note that the highest and lowest category should not be used for the generalised Hoek-Brown failure criterion.

2.4 Hoek-Brown Failure Criterion for Rock Masses

The Generalised Hoek-Brown failure criterion for rock masses is the generalised version of Equation 1 and provides a non-linear rock mass failure criterion:

$$\sigma_1' = \sigma_3' + C_0 \left(m_b \frac{\sigma_3'}{C_0} + s \right)^a \quad \textbf{(2)}$$

where m_b, s and a are unitless fitting parameters, calculated as follows (Hoek and Brown, 2018):

$$m_b = m_i \times \mathrm{e}^{\left(\frac{GSI-100}{28-14D}\right)} \quad \textbf{(3)}$$

$$s = \mathrm{e}^{\left(\frac{GSI-100}{9-3D}\right)} \quad \textbf{(4)}$$

$$a = \frac{1}{2} + \frac{1}{6}\left(e^{-\frac{GSI}{15}} - e^{-\frac{20}{3}} \right) \quad \textbf{(5)}$$

Where D is a unitless disturbance factor related to blasting damage in large excavations (Hoek and Brown, 2018). Well drilling does not use explosives that would induce damage and open the fractures, thus $D = 0$ (we provide the full equation here for completeness).

The C_0, m_i and GSI for each sandstone and granite unit were combined to solve for the rock strength (the major principal stress, σ_1') at the confining stress (the minor principal stress, σ_3') corresponding to the depths along the EPS-1 borehole according to the method in Eberhardt (2012) and Hoek and Brown (2018) using Equations 2-5.

2.5 Elastic Modulus for Rock Masses

The rock mass elastic modulus, E_{rm}, can be calculated using the Hoek-Diederichs equation (Hoek and Diederichs, 2006):

$$E_{rm} = E_i \left(0.02 + \frac{1 - D/2}{1 + e^{\left((60 + 15D - GSI)/11 \right)}} \right) \quad (6)$$

where E_i is the intact rock mass modulus obtained from uniaxial deformation experiments or estimated using the UCS (Hoek and Diederichs, 2006; Villeneuve et al., 2018).

3. RESULTS

3.1 Failure Criterion for Intact Rocks

The failure criteria for the URG granite and the dry Rehburg sandstone are shown plotted in principal stress space in Figure 3. From the triaxial testing, we derived a single C_o and m_i value for the granite: 154 MPa and 30, and multiple, unit-based C_o (see Heap et al., 2019) and a single m_i for the sandstone: 19. We combined our results and published UCS results for the URG granite to derive an average C_o of 140 MPa. The average intact elastic modulus for the granite is 40 GPa and for the dry sandstone ranges between 6-40 GPa, depending on the unit (see Heap et al., 2019). Heap et al. (2018) and Heap et al. (2019) showed that the mechanical properties of the Buntsandstein are sensitive to liquid (brine or water) saturation, however for the purposes of this paper only the dry results are presented.

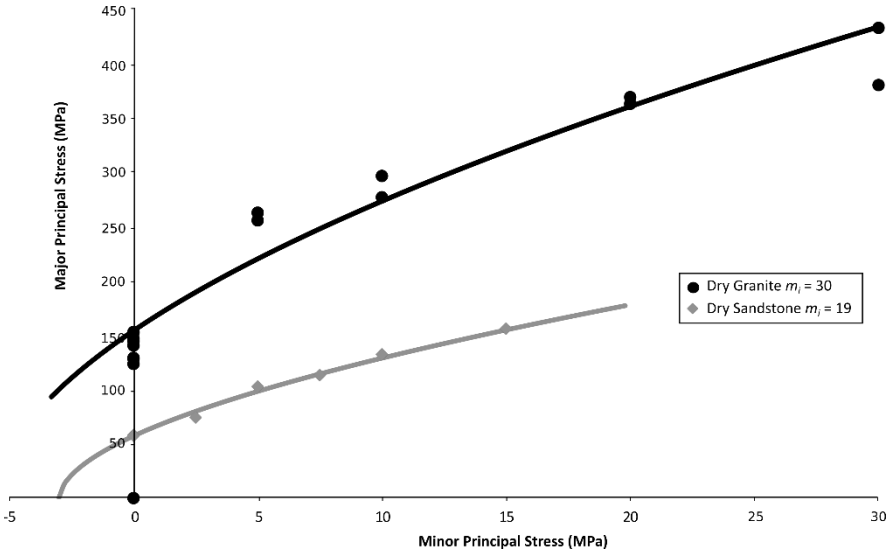

Figure 3: Triaxial and uniaxial test data with Hoek-Brown failure criterion model fits for the Soultz granite samples from 1558 m depth and the Rehberg sandstone dry samples 1239 m depth. Modified from Villeneuve et al. (2018) and Heap et al. (2019).

3.2 Depth-Corrected Strength and Stiffness Profiles for Rock Masses

For the average C_o of 140 MPa and E_i of 40 GPa in the URG granite, the rock mass strength and stiffness are lower than the intact rock strength (Figure 4B) and stiffness (Figure 4C) over all intervals with fracture frequency greater than 10 fractures/m (Figure 4A). The strength and stiffness are negatively correlated with fracture density (structure), but because GSI is a characterisation of both the structure and the surface conditions, the rock mass strength may be lower than predicted based on fracture density alone, depending on the surface conditions. In the URG, the joints with the widest aperture and thickest infilling are restricted to the most densely fractured zones, resulting in particularly low GSI in these areas (e.g. at 1450 m and 2175 m depth in Figure 4). At the wellbore scale GSI is 100 for all intervals with fracture frequency less than 10 fractures/m and therefore the rock mass strength and stiffness are the same as the intact strength and stiffness (see Villeneuve et al., 2018 for details).

The intact rock strength increases with depth, following the Hoek-Brown failure criterion (Equation 1), as shown in Figure 4B for the average C_o of 140 MPa (solid black line). The fluctuations in rock mass strength for a single C_o are more pronounced than the difference between two intact rock strengths as shown in the difference between the intact strength using the average C_o of 140 MPa (solid black line) and an upper bound C_o of 200 MPa (dashed black line). Unlike rock mass strength, values of E_{rm} do not take the influence of minor principal stress into account explicitly (Figure 4C), and do not vary with depth. Similarly to rock mass strength, rock mass stiffness fluctuates considerably with GSI, from 65% of E_i for a GSI of 75 to 3% of E_i for a GSI of 20. These low rock mass elastic modulus values are within a similar range as the wireline elastic modulus values for the fractured rock mass given in Meller and Ledésert (2017).

The full depth profile for rock mass elastic modulus for the reservoir rocks comprising the Buntsandstein and the URG granite is given in Figure 5. These data highlight, for example, that the rock mass stiffness of the granitic reservoir can be as low as or lower than that for the Buntsandstein, due to the high fracture density of the granite.

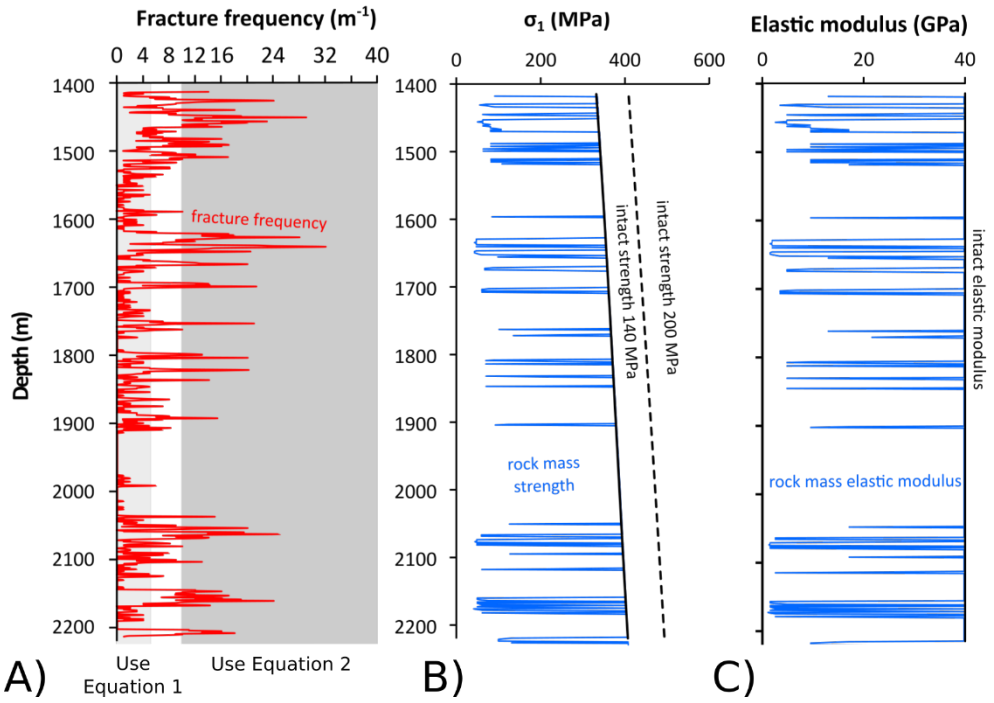

Figure 4: Comparison of A) fracture density to B) intact strength (using Equation 1 for C_o = 140 MPa (solid line) and 200 MPa (dashed line) and m_i = 30) and rock mass strength (using Equation 2) for C_o = 140 MPa and m_i = 30, and C) intact elastic modulus (E_i = 40 GPa) and rock mass elastic modulus (using Equation 6) for E_i = 40 GPa for the URG granite. Modified from Villeneuve et al. (2018).

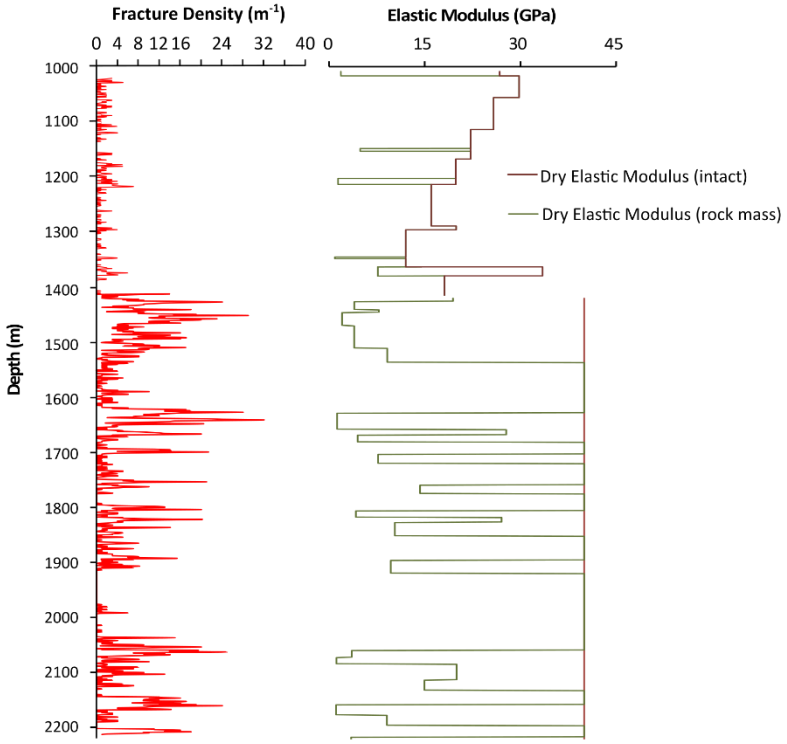

Figure 5: Fracture density data for exploration well EPS-1 at Soultz-sous-Forêts (from 1012 to 2200 m) next to the dry intact (red line) and rock mass (green line) elastic modulus. Note the contact between the Buntsandstein and the URG granite at 1440 m depth. Modified from Heap et al. (2019).

DISCUSSION AND CONCLUSIONS

We present herein a method to estimate the intact and rock mass strength and the rock mass elastic modulus of reservoir rock using easy-to-determine rock properties (uniaxial compressive strength and elastic modulus) and simple-to-use observational methods and formulae (the Hoek-Brown failure criterion and the Hoek-Diederichs equation) (Figure 6). We summarise the dry rock mass strength estimates for the URG granite at the Soultz-sous-Forêts geothermal site in France derived using this method in Villeneuve et al. (2018). We also provide rock mass elastic modulus estimates for the full sequence of reservoir rocks encompassing the Buntsandstein sedimentary sequence (from 1008 to 1414 m) and the URG granite (from 1440 m to 2200 m depth) as derived in Heap et al. (2019).

The ability to quantify the effect of macrofracturing on rock mass strength and elastic modulus provides an additional resource for interpreting and predicting well stability and reservoir behaviour. The rock mass failure criterion and elastic modulus can be used to inform the locations with optimal strength and stiffness for hydraulic stimulation. Failure criteria that incorporate the effect of macrofractures are arguably most important for the numerical modelling of fracturing, permeability and induced seismicity scenarios in reservoirs, especially where it is necessary to use continuum methods.

Thus far the generalised Hoek-Brown failure criterion has not been empirically established at the reservoir or at the wellbore scales. What we present here should be used as an estimate of lower-bound rock mass strength and stiffness, and to illustrate the impact of fractures on rock mass strength and stiffness. Most importantly we want to emphasise that using intact rock strength without consideration of the weakening and softening effect of fractures can be imprudently under-conservative. We argue that, at the reservoir scale, the effect of using only intact rock failure criteria versus using rock mass failure criteria in fractured zones to model the behaviour of the reservoir must be explored further. This is also true at the small wellbore scale.

We also show that there are many densely fractured intervals where, in our scenario, fracture density exceeds 10 fractures/m and rock mass strength and stiffness parameters should be used, even at the wellbore scale. Finally we also show that infilling type is a key aspect of rock mass characterisation, for which hematite and clay infilling information from core or wireline data is crucial. These areas are especially important to characterise because their GSI values will be particularly low. More focus on identifying fractures and infilling using wireline techniques would allow better rock mass characterisation in the absence of core.

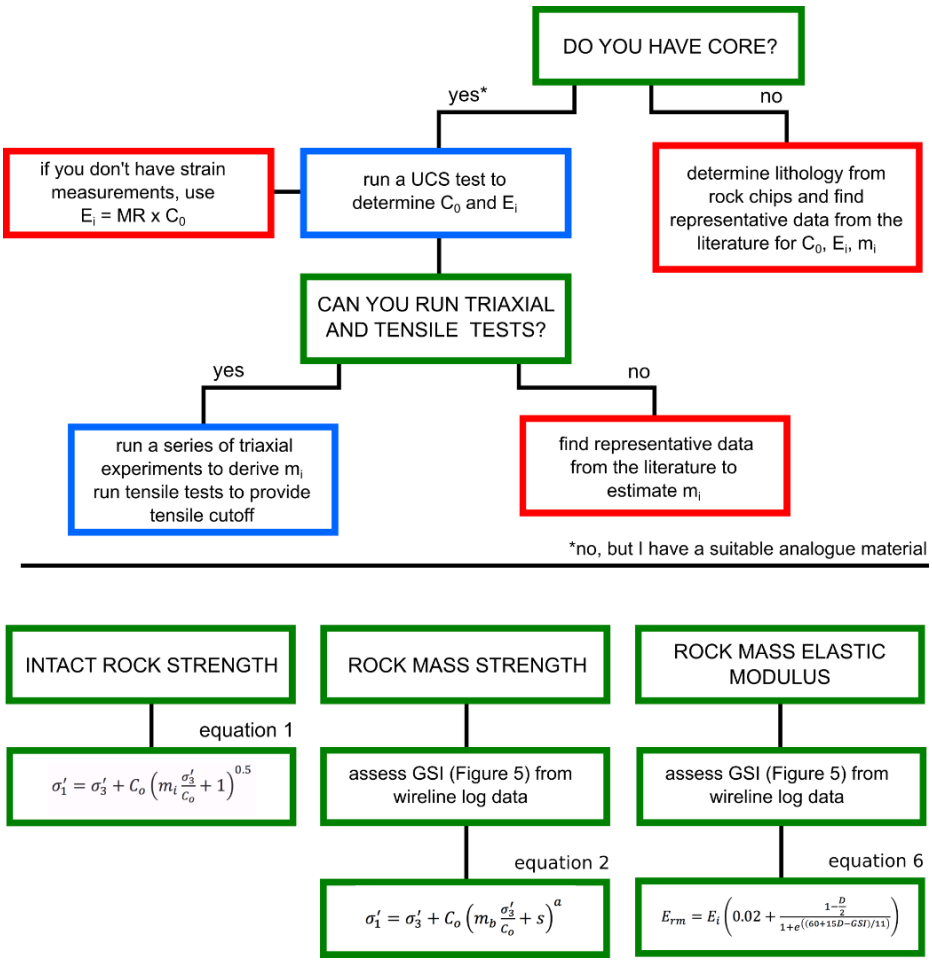

Figure 6: Flow chart for determining *in situ* strength (intact and rock mass strength) and rock mass elastic modulus depending on available data. Blue boxes show the recommended route. From Villeneuve et al. (2018).

REFERENCES

Bérard T, Cornet FH (2003) Evidence of thermally induced borehole elongation: a case study at Soultz, France. Int J Rock Mech Min Sci 40:1121–1140.

Cipolla CL, Warpinski NR, Mayerhofer MJ, Lolon EP, Vincent MC (2008) The relationship between fracture complexity, reservoir properties, and fracture treatment design. Proceedings - SPE Annual Technical Conference and Exhibition, Vol. 4, pp. 2215-2239.

Eberhardt E (2012) The Hoek–Brown failure criterion. In: R. Ulusay (ed.), The ISRM Suggested Methods for Rock Characterization, Testing and Monitoring: 2007–2014:233-240.

Genter A, Traineau H (1996) Analysis of macroscopic fractures in granite in the HDR geothermal well EPS-1, Soultz-sous-Forêts, France. J Volcanol Geotherm Res 72(1-2):121-141.

Griffiths L, Heap MJ, Wang F, Daval D, Gilg HA, Baud P, Schmittbuhl J, Genter A. (2016) Geothermal implications for fracture-filling hydrothermal precipitation. Geothermics 64, 235-45.

Guillou-Frottier L, Carré C, Bourgine B, Bouchot V, Genter A (2013) Structure of hydrothermal convection in the Upper Rhine Graben as inferred from corrected temperature data and basin-scale numerical models. J Volcanol Geotherm Res 256:29-49.

Heap MJ, Kushnir ARL, Gilg HA, Wadsworth FB, Reuschlé T, Baud P (2017) Microstructural and petrophysical properties of the Permo-Triassic sandstones (Buntsandstein) from the Soultz-sous-Forêts geothermal site (France). Geotherm Energy 5(1):26.

Heap MJ, Reuschlé T, Kushnir ARL, Baud P (2018) The influence of hydrothermal brine on the short-term strength and elastic modulus of sandstones from exploration well EPS-1 at Soultz-sous-Forêts (France). Geotherm Energy 6(1):29.

Heap M, Villeneuve M, Kushnir A, Farquharson J, Baud P, Reuschlé T (2019) Rock mass strength and elastic modulus of the Buntsandstein: An important lithostratigraphic unit for geothermal exploitation in the Upper Rhine Graben. Geothermics 77, 236–256.

Hoek E, Brown ET. (1980) Empirical Strength Criterion for Rock Masses. J Geotech Geoenviron Eng 106 (GT9):1013-1035.

Hoek E, Brown ET (2018) The Hoek–Brown failure criterion and GSI – 2018 edition. Journal of Rock Mechanics and Geotechnical Engineering, 11(3):445-463.

Hoek E, Diederichs MS (2006) Empirical estimation of rock mass modulus. Int J Rock Mech Min Sci 43(2):203-215.

Kushnir ARL, Heap MJ, Baud P (2018) Assessing the role of fractures on the permeability of the Permo-Triassic sandstones at the Soultz-sous-Forêts (France) geothermal site. Geothermics 74:181-189.

Magnenet V, Fond C, Genter A, Schmittbuhl J(2014) Two-dimensional THM modelling of the large scale natural hydrothermal circulation at Soultz-sous-Forêts. Geotherm Energy 2(1):17.

Marinos V, Marinos P, Hoek E (2005) The geological strength index: applications and limitations. Bull Eng Geol Environ 64:55-65.

McClure M, Horne RN (2013) Discrete fracture network modeling of hydraulic stimulation: Coupling flow and geomechanics. Springer Science & Business Media. doi: 10.1007/978-3-319-00383-2.

Meller C, Ledésert B (2017) Is there a link between mineralogy, petrophysics, and the hydraulic and seismic behaviors of the Soultz-sous-Forêts granite during stimulation? A review and reinterpretation of petro-hydromechanical data toward a better understanding of induced seismicity and fluid flow. Journal of Geophysical Research: Solid Earth 122:9755–9774.

Pribnow D, Schellschmidt R (2000) Thermal tracking of upper crustal fluid flow in the Rhine Graben. Geophys Res Lett 27(13):1957-1960.

Richards L, Read S (2007) New Zealand greywacke characteristics and influence on rock mass behavior. The Second Half Century of Rock Mechanics. 11th Congress of the International Society for Rock Mechanics, Lisbon. Taylor & Francis, London.

Villeneuve M, Heap M, Kushnir A, Qin T, Baud P, Zhou G, Xu T (2018) Estimating in situ rock mass strength and elastic modulus of granite from the Soultz-sous-Forêts geothermal reservoir (France). Geotherm Energy 6(11).

Yoon JS, Zang A, Stephansson O (2014) Numerical investigation on optimized stimulation of intact and naturally fractured deep geothermal reservoirs using hydro-mechanical coupled discrete particles joints model. Geothermics 52:165-184.